

6-2016

Micropaleontology of the 2013 Typhoon Haiyan Overwash Sediments from the Leyte Gulf, Philippines

Jessica E. Pilarczyk

Benjamin P. Horton

Janneli Lea A. Soria

Adam D. Switzer

Fernando Siringan

See next page for additional authors

Authors

Jessica E. Pilarczyk, Benjamin P. Horton, Janneli Lea A. Soria, Adam D. Switzer, Fernando Siringan, Hermann M. Fritz, Nicole S. Khan, Sorvigenaleon Ildefonso, Angelique A. Doctor, and Mikko L. Garcia

1 Micropaleontology of the 2013 Typhoon Haiyan
2 overwash sediments from the Leyte Gulf, Philippines

3

4 Jessica E. Pilarczyk^{1,2,3}, Benjamin P. Horton^{1,3}, Janneli Lea A. Soria^{3,4}, Adam D.
5 Switzer^{3,4}, Fernando Siringan⁵, Hermann M. Fritz⁶, Nicole S. Khan¹, Sorvigenaleon
6 Ildefonso³, Angelique A. Doctor⁵, Mikko L. Garcia⁵

7

8 ¹Department of Marine and Coastal Science and Institute of Earth, Ocean, &
9 Atmospheric Sciences, Rutgers University, New Brunswick, NJ 08901, USA

10 ²Department of Marine Science, University of Southern Mississippi, Stennis Space
11 Center, MS 39529, USA

12 ³ Earth Observatory of Singapore, Nanyang Technological University, Singapore

13 ⁴Asian School of the Environment, Nanyang Technological University, Singapore

14 ⁵ University of Philippines – Diliman, Quezon City, Philippines

15 ⁶ School of Civil and Environmental Engineering, Georgia Institute of Technology,
16 Atlanta, GA 30332, USA

17

18 *Abstract*

19 Coastal geologic records allow for the assessment of long-term patterns of
20 tropical cyclone variability. However, the accuracy of geologic reconstructions of
21 tropical cyclones is limited by the lack of modern analogues. We describe the
22 microfossil (foraminifera and testate amoebae) assemblages contained within
23 overwash sediments deposited by Typhoon Haiyan when it made landfall on the
24 islands of Leyte and Samar in the Philippines on 7 November 2013 as a category
25 5 super typhoon. The overwash sediments were transported up to 1.7 km inland

26 at four study sites. The sediments consisted of light brown medium sand in a
27 layer <1 to 8 cm thick. We used Partitioning Around a Medoid (PAM) cluster
28 analysis to identify lateral and vertical changes in the foraminiferal and testate
29 amoebae data. The presence of intertidal and subtidal benthic, and planktic
30 foraminifera that were variably unaltered and abraded identify the microfossil
31 signature of the overwash sediments. Agglutinated mangrove foraminifera and
32 testate amoebae were present within the overwash sediments at many locations
33 and indicate terrestrial scouring by Haiyan's storm surge. PAM cluster analysis
34 subdivided the Haiyan microfossil dataset into two assemblages based on
35 depositional environment: (1) a low-energy mixed-carbonate tidal flat located on
36 Samar Island (Basey transect); and (2) a higher-energy clastic coastline near
37 Tanauan on Leyte Island (Santa Cruz, Solano, and Magay transects). The
38 assemblages and the taphonomy suggest a mixed provenance, including
39 intertidal and subtidal sources, as well as a contribution of sediment sourced
40 from deeper water and terrestrial environments.

41 Keywords

42 Tropical cyclone; Overwash; Foraminifera; Testate amoebae; Sediments;
43 Paleotempestology

44

45 *1. Introduction*

46 Landfalling tropical cyclones pose a hazard to the concentrations of
47 population, economic production, and static infrastructure along the coastlines
48 of the Philippines. The Philippines are in close proximity to the Main
49 Development Region (MDR) in the North Pacific (Pun et al., 2013), which is the
50 most active tropical cyclone region in the world (Lin et al., 2013). Numerous
51 tropical cyclones have made landfall on the Philippines (e.g., Typhoon Agnes in
52 1984, Typhoon Mike in 1990, Typhoon Thelma in 1991, and Typhoon Hagupit in
53 2014; e.g., Garcia-Herrera et al., 2007; Ribera et al., 2008; NDRRMC, 2014),

54 including Typhoon Haiyan, which was one of the most intense storms on record.
55 Despite the history of typhoon activity in the Philippines, we lack an
56 understanding of the role of recent warming on tropical cyclone activity because
57 of the length of the instrumental record (Landsea et al., 2006). Fortunately,
58 proxy records of overwash sediments are transforming our ability to detect and
59 analyze the underlying climatic forcing for tropical cyclone activity over the last
60 several millennia (Lane et al., 2011; Brandon et al., 2013; Denommee et al., 2014;
61 Donnelly et al., 2015).

62 Storm surges associated with past tropical cyclones deposit overwash
63 sediments that become preserved in the geologic record. The identification of
64 overwash sediments is commonly based on the recognition of anomalous sand
65 layers in otherwise low-energy coastal settings (e.g., Liu and Fearn, 1993, 2000;
66 Donnelly et al., 2001) supported by microfossils, which can indicate provenance
67 of sediment (e.g., Collins et al., 1999; Hippensteel and Martin, 1999; Scott et al.,
68 2003; Hippensteel et al., 2005; Hawkes and Horton, 2012). Marine microfossils,
69 such as foraminifera, are often present in overwash sediments due to the
70 landward transport and deposition of coastal and marine sediment during a
71 tropical cyclone's storm surge (e.g., Hippensteel and Martin, 1999; Scott et al.,
72 2003; Lane et al., 2011). Testate amoebae are commonly found in freshwater
73 environments (e.g., Ogden and Hedley, 1980; Charman, 2001; Smith et al., 2008)
74 and have potential as indicators of terrestrial scouring by a storm surge.

75 An obstacle in identifying past tropical cyclones in the geologic record is
76 the lack of a modern analogue. However, the microfossil signature of modern
77 tropical cyclone overwash sediments can provide insight into their long-term
78 preservation in the fossil record (Otvos, 1999; Scott et al., 2003; Hippensteel et
79 al., 2005), and can be directly compared to similar studies of overwash
80 sediments deposited by tsunamis (Dominey-Howes et al., 2000; Hawkes et al.,
81 2007; Clark et al., 2011; Goff et al., 2011; Pilarczyk et al., 2012). The majority of
82 studies that employ foraminifera to document tropical cyclone sediments have
83 been conducted in temperate environments from the Atlantic Ocean (Scott et al.,

84 2003; Kortekaas and Dawson, 2007; Hippensteel et al., 2013) and Gulf of Mexico
85 (Williams, 2009; Hawkes and Horton, 2012; Rabien et al., 2015), with little
86 research in tropical or semi-tropical environments (Strotz and Mamo, 2009;
87 Pilarczyk and Reinhardt, 2012) such as the Philippines.

88 In this paper we document the microfossil assemblages of the Typhoon
89 Haiyan overwash sediments, collected less than two months after the storm
90 made landfall on 7 November 2013. A series of trenches and cores was obtained
91 at four sites from two contrasting environments (one mixed-carbonate site and
92 three clastic sites) along the northwestern Leyte Gulf coastline (Fig. 1). Haiyan
93 sediments were discriminated from underlying pre-storm sediments by the
94 presence of intertidal and subtidal benthic, and planktic foraminifera. The
95 unaltered (i.e., pristine) and abraded nature of the foraminifera within the
96 Haiyan overwash sediments point to a mixed provenance, including terrestrial,
97 intertidal, subtidal, and deeper sources. Evidence of terrestrial scour by the
98 storm surge is indicated by the presence of agglutinated mangrove foraminifera
99 and freshwater testate amoebae. The microfossil signature of the overwash
100 sediments deposited by Typhoon Haiyan serves as the only modern analogue of
101 a landfalling typhoon in the Philippines, and may be important to the recognition
102 and interpretation of older storm sediments preserved in coastal sequences at
103 this location, as well as other tropical settings worldwide.

104

105 *2. Typhoon Haiyan*

106 Typhoon Haiyan (locally known as Yolanda) was the thirtieth named
107 storm in the 2013 Pacific typhoon season. Haiyan began as a westward-tracking
108 low-pressure system on 2 November that developed into a tropical storm by
109 0000 UTC on 4 November and rapidly intensified to typhoon intensity eight
110 hours later (Joint Typhoon Warning Center, 2014; Fig. 1a). By 7 November, the
111 Joint Typhoon Warning Centre (JTWC) reported gusts of up to 314 km/h three
112 hours before initial landfall and declared the storm a Category 5, designating

113 Typhoon Haiyan as one of the most intense tropical cyclones. At 2040 UTC on 7
114 November, Haiyan made its first landfall over Guiuan, Eastern Samar and
115 continued west-northwest across the Leyte Gulf where it made its second
116 landfall over Tolosa and the Greater Tacloban area at 2300 UTC (Fig. 1b).
117 Following six landfalls in the Philippines (Guiuan and Tacloban in Leyte;
118 Daanbantayan and Bantayan in Cebu; Concepcion in Iloilo; and Busuanga in
119 Palawan), Haiyan weakened to a Category 2 before striking northeastern
120 Vietnam at 0000 UTC on 8 November, after which the storm tracked northeast
121 and dissipated over China (Fig. 1a).

122 Typhoon Haiyan was associated with severe rainfall (491 mm) and high
123 wind speeds (10 minute sustained wind speed of 230 km/hr), but most of the
124 damage was caused by the 5 to 7 m high storm surge (Mori et al., 2014; Nguyen
125 et al., 2014; Tajima et al., 2014; Soria et al., 2016b). The coastlines of the Leyte
126 Gulf sustained the greatest impact, with destruction centered near Tacloban,
127 which sits less than 5 m above mean sea level (MSL). Storm surge heights
128 (elevation of terrain + flow depth above terrain) and inundation distances
129 (inland extent of marine incursion) from coastlines surrounding the Leyte Gulf
130 (including our four study sites) are presented in Soria et al. (2016b).

131

132 *3. Site description*

133 The Leyte Gulf, ~580 km southeast of the capital city Manila, is bordered
134 by two islands separated by the narrow San Juanico Strait, Leyte Island to the
135 west, and Samar Island to the north and east (Fig. 1). The seismically active
136 Philippine Fault bisects Leyte Island, which is made up of Pliocene-Quaternary
137 volcano cones and Tertiary volcanoclastic rocks and sediments (Allen, 1962;
138 Duquesnoy et al., 1994). Quaternary alluvium, consisting of unconsolidated,
139 poorly sorted sands (Travaglia et al., 1978; Suerte et al., 2005) characterizes the
140 Leyte Gulf side of Samar Island. Sediment inputs to the northern Leyte Gulf

141 include biogenic sediments in reef areas, littoral sediment transported by waves,
142 terrigenous material transported by high rainfall through rivers (e.g., clastics and
143 volcanic residuals; Hart et al., 2002), and deeper offshore sediment carried
144 landward by storms.

145 Our study focused on a series of four transects from two islands: Basey
146 (Ba) on Samar Island; and the Tanauan transects (Santa Cruz, Sc; Solano, So; and
147 Magay, Ma) on Leyte Island (Fig. 1 c,d). The coastline at Basey is characterized by
148 a low-energy mixed-carbonate tidal flat. A gently sloping, narrow sandy beach is
149 present, but was heavily eroded by Typhoon Haiyan. Coconut groves and rice
150 fields are found landward of the beach. The Tanauan coastline is characterized
151 by a higher-energy, wave dominated system. The coastline is a broad, gently
152 sloping coastal plain that is drained by the Embarcadero River (Fig. 1d) and
153 consists of a mixture of siliciclastic and volcanoclastic sediments. The beach at all
154 three Tanauan transect sites was also heavily eroded by Typhoon Haiyan, with
155 coconut groves, ponds, and rice fields occurring farther landward (Fig. 1d;
156 Supplementary Fig. S1). At Magay, *Nypa fruticans* Wurmb, a species of palm
157 adapted to mangrove environments, is found in water-logged and densely
158 vegetated patches that are associated with incised intertidal channels.

159 The transects at Samar and Leyte Islands were located in regions that
160 were impacted by high storm surges (Soria et al., 2016b) and experienced
161 minimal anthropogenic alteration in the weeks following Haiyan's landfall.
162 Three closely spaced transects near Tanauan were chosen to assess variability
163 within the overwash sediments. The transects extend from the shoreline to the
164 landward limit of the Haiyan overwash sediments. We attempted to sample the
165 full coastal gradient from the shoreline to the Haiyan inundation limit, however,
166 storm damage (e.g., flooding, destroyed roads) prevented the survey team from
167 accessing certain areas.

168

170 In January 2014, we collected sediments from our four transects (Fig. 1b).
171 A detailed lithostratigraphic investigation was completed along each transect
172 from a series of sampling stations. Samples were collected using a hand gouge
173 corer or by excavating shallow trenches. The location of all sampling stations
174 was determined by handheld GPS. At each station we collected one sediment
175 sample from the midpoint (if available) of the Haiyan sediments and one sample
176 from the underlying sediment. At three stations (spaced 50 m apart) within the
177 *Nypa* forest at Magay (transect Ma), where the Haiyan sediments were exposed
178 at the surface, we dug shallow trenches (Ma4, Ma6, and Ma9; Fig. 1d). The
179 trenches were sampled every 1 cm within the Haiyan sediments and two
180 samples were obtained from the underlying sedimentary layer. Samples were
181 sealed in plastic wrap, and held in refrigerated storage until processing.

182 At Basey on Samar Island, we collected sediments along a shore normal
183 transect (Ba) consisting of 15 gouge cores (Ba1 to Ba18; Ba 6, 16, and 17 were
184 not sampled) from the beach (0 - 30 m along the transect), coconut grove (30 -
185 210 m) and rice field (210 - 360 m) environments (Fig. 1c). At the Santa Cruz
186 site we collected sediments along a shore normal transect (Sc) consisting of 8
187 gouge cores (Sc1 to Sc8) that extended from the beach (0 - 10 m), to a low-lying
188 grassy area with ponds (10 - 530 m), to a rice field (550 - 890 m). At Solano,
189 sediments were obtained from a shore normal transect (So) that consisted of 13
190 gouge cores (So1 to So13) from several environments including: an extensive,
191 low-lying grassy area interspersed with shallow ponds (260 - 1400 m), a rice
192 field (1400 - 1600 m), and a coconut grove (≥ 1600 m). At Magay we collected
193 sediments along a shore normal transect (Ma) consisting of 5 gouge cores (Ma1,
194 Ma2, Ma10-12) and three trench sections (Ma4, Ma6, Ma9) that extended from
195 the shoreline (0 - 20 m), to a low-lying grassy area (20 - 120 m), to a fringing
196 *Nypa* forest (120 - 540 m), to a rice field (1100 - 1690 m; Fig. 1d). The transect
197 extended through the village of Magay (between 540 m and 1100 m), which

198 consisted of several dozen homes and buildings before the typhoon made
199 landfall.

200 We conducted microfossil analysis on all core and trench samples. For
201 microfossil analysis, 5 cm³ sediment samples were washed over a 32 µm sieve to
202 retain foraminifera (intertidal to marine organisms) and testate amoebae
203 (freshwater organisms) tests, and wet split to obtain counts of ~300 specimens.
204 Foraminiferal taxonomy followed Loeblich and Tappan (1987), Debenay (2013),
205 and Hayward et al. (2004), and species identification was confirmed using the
206 Cushman Collection of Foraminifera at the National Museum of Natural History,
207 Smithsonian Institute. We interpreted the foraminiferal data in relation to
208 studies by Glenn-Sullivan and Evans (2001), Hewins and Perry (2006), Lacuna et
209 al. (2013), and Lacuna and Alviro (2014), that examined modern foraminifera
210 from select coastal zones throughout the Philippines. Testate amoebae were
211 identified to the genus level using Ogden and Hedley (1980). Foraminifera (both
212 calcareous and agglutinated species) were divided into small (<250 µm) and
213 large (>250 µm) test sizes by means of sieving. Calcareous species were
214 categorized using the same taphonomic criteria defined by Pilarczyk et al.
215 (2011), which includes: unaltered, abraded (including corroded and edge
216 rounded specimens), and fragmented forms (Fig. 2). An individual foraminifera
217 can be both abraded and fragmented. The taphonomic condition of individual
218 foraminifera has previously been used to interpret overwash sediments by
219 assessing depth of scour and origin of sediment (e.g., Goff et al., 2011; Pilarczyk
220 et al., 2012). All microfossil results are listed in Supplementary Tables S1 – S4.

221 We used Partitioning Around a Medoid (PAM) cluster analysis (Kaufman
222 and Rousseeuw, 1990) of the relative abundance of foraminiferal and testate
223 amoebae assemblages and taphonomic characteristics to discriminate the
224 Haiyan overwash sediments from underlying sediment. PAM cluster analysis
225 was also used to identify lateral changes in overwash sediments at Basey and
226 Tanauan. Only categories with a minimum abundance of 5% in at least one
227 sample were used in cluster analysis. Abundances were then used to calculate z-

228 scores. Z-scores are a means of standardizing datasets by assessing how many
229 standard deviations a value is from the mean. A z-score of 0 indicates the value
230 is the same as the mean; whereas, a positive or negative score indicates how
231 many standard deviations the value is above (positive score) or below (negative
232 score) the mean. We performed PAM cluster analysis following the methods of
233 Kemp et al. (2012), using the 'cluster' package in R (Maechler et al., 2005).
234 Silhouette plots generated by PAM range in width from -1 to 1 and are an
235 estimate of a sample's classification, where values close to -1 are those that are
236 incorrectly classified, and those close to 1 indicate assignment to an appropriate
237 cluster. We used the maximum average silhouette width to determine the
238 number of clusters within each of our cluster scenarios.

239 *5. Results*

240 *Basey Transect (Ba)*

241 The Typhoon Haiyan surge height at Basey was up to 6.5 m above MSL
242 (Soria et al., 2016b). Inundation reached at least 1 km inland, whereas the
243 corresponding overwash sediments were only found up to 360 m. The Haiyan
244 overwash sediments consist of medium to fine sand and, where present, range
245 in thickness from 8 cm closest to the shoreline to <1 cm in the rice fields
246 (Supplementary Table S1). The overwash sediments are light brown (10 YR 7/2)
247 in color and carbonate-rich, containing foraminifera and fragments of corals and
248 mollusks that are similar to those found in modern nearshore and beach
249 sediments. The Haiyan sediments overlie either coconut grove or rice field soils
250 with a sharp stratigraphic contact. However, at the time of sampling, post-
251 typhoon vegetation growth in the rice fields (i.e., Supplementary Fig. S1c) had
252 already begun to obscure the contact.

253 The Haiyan overwash sediments at Basey contain abundant foraminifera.
254 Concentrations of foraminifera are highest at sample sites closest to the
255 shoreline (up to 6320 foraminifera per 5 cm³), and begin to markedly decrease

256 beginning at ~100 m inland, where concentrations decrease to 45 foraminifera
257 per 5 cm³ (Fig. 3; Supplementary Table S1). The Haiyan assemblage consists
258 exclusively of calcareous species such as *Ammonia tepida* (Cushman, 1926; 4 –
259 47%), *Ammonia convexa* Collins 1958 (0 – 22%), and *Pararotalia* sp. (2 – 20%;
260 Fig. 2). Planktic foraminifera are present in the overwash sediments at all
261 sampled locations (<2%) except where total concentration is very low (Ba9,
262 Ba18, and Ba1). Unaltered deeper-dwelling species such as *Eponides repandus*
263 (Fichtel and Moll, 1798; up to 13%) and *Cibicides tabaensis* Perelis and Reiss
264 (1976; 0 – 2%) are also present, but in lower abundances. Testate amoebae are
265 absent from the overwash sediments except at sites landward of Ba3 (190 m
266 from the shoreline), where *Diffugia* spp. are present (3 - 63%). The taphonomic
267 condition of foraminifera within the Haiyan sediments includes unaltered,
268 abraded, and fragmented forms. Samples within 150 m of the shoreline are
269 generally dominated by abraded individuals (29 – 66%; Supplementary Table
270 S1) with a large test (>250 μm) size (43 – 71% of tests). Beginning at ~170 m
271 inland (Ba7), unaltered individuals (38 – 64%) with a small test (<250 μm) size
272 (59 – 100% of tests) generally dominate the assemblage.

273 Foraminifera were absent from underlying soil units at all sites except
274 Ba13, Ba14, and Ba18 in the coconut grove. The total concentration of
275 foraminifera in these soils was lower than in the overlying Haiyan sediments
276 (e.g., 125 foraminifera per 5 cm³ in underlying soils vs. 6320 foraminifera per 5
277 cm³ in Haiyan sediments at Ba14). The taxonomic assemblage of the soil
278 consists of nearshore species including *A. convexa* (18 – 26%), *Ammonia*
279 *parkinsoniana* (d’Orbigny, 1839; 6 – 25%), and *Elphidium striatopunctatum*
280 (Fitchel and Moll, 1798; 25 – 36%). Testate amoebae (*Diffugia* spp.) are found
281 at Ba3 (inland extent of the coconut grove) and the rice fields (145 – 1110 per 5
282 cm³). Foraminifera within the soil units are dominantly abraded (82 – 100%)
283 and small sized (79 – 95%).

284

286 The surge height recorded at Santa Cruz on Leyte Island reached 5.1 m
287 above MSL and inundated up to 3 km inland (Soria et al., 2016b), however, we
288 could only trace the corresponding sedimentary deposit up to 890 m. The
289 Haiyan overwash sediments at Santa Cruz were characterized by a patchy,
290 medium to fine sand (Soria et al., 2016a), variable thickness (<1 – 7 cm;
291 Supplementary Table S2), a light brown color (10 YR 7/2), and the presence of
292 siliciclastic and volcanoclastic sediments. The overwash sediments overlie either
293 grassy soil, pond sediment, or rice field soil with a gradational contact resulting
294 from post-typhoon bioturbation.

295 Foraminiferal concentrations within the overwash sediments at Santa
296 Cruz are lower than those observed at Basey (e.g., 5 - 35 individuals per 5 cm³ at
297 Santa Cruz vs. 45 – 6320 individuals per 5 cm³ at Basey; Fig. 4a; Supplementary
298 Table S2). Similar to Basey, concentrations of foraminifera are highest at sample
299 sites closest to the shoreline (e.g., 25 - 35 foraminifera per 5 cm³ within 20 m of
300 the shoreline), and lowest at the furthest inland sites (5 – 20 foraminifera per 5
301 cm³ from 440 – 890 m). The Haiyan assemblage at Santa Cruz is dominated by
302 benthic and planktic calcareous foraminifera. *Ammonia convexa* (0 – 33%), and
303 *A. parkinsoniana* (0 – 31%) are the most dominant benthic species (Fig. 4a).
304 Planktics (9 – 24%) are present at all sites except Sc1 located closest to the
305 shoreline. In general, testate amoebae, including *Diffugia* spp. (up to 73%) and
306 *Centropyxis* spp. (up to 30%), are abundant within the overwash sediments (Fig.
307 2). The taphonomic condition of foraminifera within the overwash sediments
308 includes unaltered (22 – 73%), abraded (17 – 78%), and fragmented (16 – 51%)
309 forms. The concentration of unaltered individuals at Santa Cruz exceeded
310 abraded and fragmented individuals at all locations except Sc1 and Sc5. In
311 contrast to Basey, the abundance of unaltered individuals was unrelated to
312 distance inland. Similarly, there was no observable relationship between test
313 size and distance inland. Larger foraminifera dominate sites Sc1 – Sc2 and Sc5 –

314 Sc6 (57 – 66%), whereas smaller foraminifera dominate sites Sc3 – Sc4 and Sc7 –
315 Sc8 (57 – 68%).

316 Foraminifera were absent in all underlying soils. However, pond
317 sediment (120 testate amoebae per 5 cm³), as well as grass (25 - 75 testate
318 amoebae per 5 cm³), and rice field (1025 - 1270 testate amoebae per 5 cm³) soils
319 contained abundant *in situ* testate amoebae. The soil underlying the grassy area
320 at Sc1 and Sc2, closest to the shoreline, is dominated by *Centropyxis* spp. (54 –
321 75%). At a distance of 440 m inland, the assemblage switches to one that is
322 dominated by *Diffugia* spp. (85 – 93%).

323 *Solano Transect (So)*

324 We were unable to measure the Typhoon Haiyan surge height at Solano,
325 however it would have been similar to the surge heights measured a few
326 hundred meters shoreward at Santa Cruz (5.1 m above MSL) and Magay (5.4 m
327 above MSL). At Solano, the overwash sediments reached a distance of 1.6 km
328 inland, which is less than the 2.8 km inundation distance reported by Soria et al.
329 (2016b). The overwash sediments at Solano consisted of a patchy fine to
330 medium sand (Soria et al., 2016a) with variable thickness (<1 – 4.5 cm;
331 Supplementary Table S3), a light brown color (10 YR 7/2), and the presence of
332 siliciclastic and volcanoclastic sediments. A sharp contact between the overwash
333 sediments and the underlying soil was observed at all sites except those located
334 within the rice fields where bioturbation by roots has resulted in a gradational
335 contact.

336 The total concentration of foraminifera within the overwash sediments at
337 Solano is similar to concentrations observed at Santa Cruz (ranging from 10 – 80
338 individuals per 5 cm³; Fig. 4b; Supplementary Table S3). Similarly, the species
339 contained within the overwash sediments are similar at both sites, where
340 shallow intertidal to subtidal benthics as well as planktics dominate the
341 assemblage. *Ammonia convexa* (0 – 27%) and *A. parkinsoniana* (0 – 20%) are

342 generally the most dominant benthic species (Fig. 2; Fig. 4b). Planktics are found
343 throughout the overwash sediments (4 – 33%), including at So13 (10%) located
344 at a distance of 1.6 km inland. Testate amoebae are also present within the
345 overwash sediments at Solano (up to 93% of the Haiyan assemblage). The
346 foraminiferal taphonomic assemblage within the overwash sediments switched
347 at 460 m inland from one that is generally dominated by fragmented individuals
348 (e.g., 54% at So5) to one that is dominated by unaltered individuals (e.g., 100%
349 at So13, 1.6 km from the shoreline). At Solano, test size generally decreased with
350 increasing distance inland (e.g., 45% of foraminifera were small at So1 compared
351 to 82% at So12). Small foraminifera were more abundant in the overwash
352 sediments than larger ones except at So1, closest to the shoreline (45% small vs.
353 55% large), and So6 in the coconut grove (37% small vs. 63% large).

354 The underlying soils at Solano are devoid of foraminifera, but contain
355 testate amoebae, except at the coconut grove sites (So12 and So13). Total
356 concentrations of testate amoebae are generally higher in the soils of rice fields
357 (5960 – 11,475 per 5 cm³) than in the soils/sediments associated with grassy
358 areas (135 - 280 per 5 cm³), ponds (1250 per 5 cm³), and coconut groves (0 – 65
359 per 5 cm³). *Centropyxis* spp. dominates the grassy area between 260 m and 290
360 m (58 – 70%), and beginning at 290 m inland, the assemblage switches to one
361 that is dominated by *Diffflugia* spp. (60 – 93%).

362

363 *Magay Transect (Ma)*

364 The surge height recorded at Magay on Leyte Island reached 5.4 m above
365 MSL and 2.0 km inland (Soria et al., 2016b). However, we could only trace the
366 deposit up to 1.7 km. The overwash sediments at Magay are characterized by a
367 patchy, medium to fine sand (Soria et al., 2016a), variable thicknesses (<1 – 7
368 cm; Supplementary Table S4), a light brown color (10 YR 7/2), and the presence
369 of siliciclastics and volcanoclastics. The contact between the overwash sediments

370 and the underlying soil was sharp in the *Nypa* forest, but gradational at all other
371 locations due to bioturbation by roots.

372 Foraminiferal concentrations within the overwash sediments at Magay
373 are similar to those from Santa Cruz and Solano and range from 15 to 150
374 individuals per 5 cm³ (Fig. 5a,b; Supplementary Table S4). The overwash
375 sediments consist of benthic and planktic foraminifera that are both calcareous
376 and agglutinated. In general, *Ammonia parkinsoniana* (6 – 57%), and planktic
377 species (0 – 87%) dominate the Haiyan assemblage. In contrast to all other sites,
378 the Haiyan assemblage at Magay also contains agglutinated mangrove
379 foraminifera. Agglutinated foraminifera are limited to sample locations within
380 the *Nypa* forest (Ma4, Ma6, and Ma9; Supplementary Table S4) and include
381 *Trochammina inflata* (Montagu, 1808; 0 – 29%), *Miliammina fusca* (Brady, 1870;
382 0 – 27%), *Haplophragmoides wilberti* Andersen, 1953 (0 – 23%), *Entzia*
383 *macrescens* (Brady, 1870; 0 – 22%), and *Ammobaculites* sp. (0 – 17%). Testate
384 amoebae are also found within the overwash sediments at sites within the rice
385 field, where *Diffugia* spp. dominate (37 – 50%), as well as Ma9 (*Nypa* forest),
386 where the testate amoebae assemblage of the overwash sediments is comprised
387 exclusively of *Centropyxis* spp. (up to 27% of the total microfossil assemblage;
388 Fig. 2). The taphonomic assemblage of the overwash sediments is dominated by
389 unaltered individuals (29 – 82%) up to a distance of 1.4 km inland, at which
390 point the assemblage switches to one that is dominated by abraded forms (e.g.,
391 75% of foraminifera at Ma12 are abraded). In general, the test size of
392 foraminifera observed at Ma decreased with increasing distance inland (e.g.,
393 64% large sized foraminifera at Ma2 vs. 14% at Ma12).

394 Soils underlying the *Nypa* forest (Ma4, Ma6, and Ma9) contained
395 agglutinated foraminifera that comprised 90 – 100% of the total microfossil
396 assemblage (Fig. 5). Testate amoebae are present within underlying soils from
397 the grassy area (69 – 100% *Centropyxis* spp.), the rice fields (74 – 76% *Diffugia*
398 spp.), and to a lesser extent, within the *Nypa* (e.g., 4 – 9% testate amoebae at
399 Ma9). The trench stations at Ma4, Ma6, and Ma9 (sampled every 1 cm) show no

400 relationship between total concentration and depth within the overwash
401 sediments (Fig. 5b; Supplementary Table S4). However, concentrations were
402 significantly lower in the overwash sediments compared to the underlying soil
403 (e.g., 35 – 70 vs. 325 – 905 foraminifera per 5 cm³ respectively at Ma9). The
404 Haiyan assemblage in trench samples was dominated by planktic foraminifera
405 (up to 87%), with agglutinated mangrove species found at the lower and upper
406 contacts of the deposit. The taphonomic assemblage of the overwash sediments
407 within trench sections was dominated by unaltered individuals (e.g., 50 – 69% of
408 the assemblage at Ma4), but did not show any relationship with depth. Test size
409 showed a relationship with depth at trench Ma4, where larger foraminifera
410 (>250 µm) were concentrated at the base of the overwash sediments (66% large
411 at the base vs. 30% large at the top).

412

413 *Cluster analysis*

414 We used PAM cluster analysis to classify the microfossil signature of the
415 overwash sediments and to assess lateral changes in the foraminiferal (relative
416 abundance, total concentration, taxonomy, taphonomy, and test size) and testate
417 amoebae data. PAM cluster analysis distinguished Haiyan sediments from the
418 underlying soil (Fig. 6a). Cluster A1 (average silhouette width = 0.005) generally
419 consisted of Haiyan sediments that are composed of calcareous foraminifera (5 –
420 6320 foraminifera per 5 cm³); whereas cluster A2 (average silhouette width =
421 0.737) contained only underlying soil samples that were generally devoid of
422 calcareous foraminifera. The underlying soils at Ba13, 14, and 18 clustered in A1
423 due to the presence of low abundances of calcareous foraminifera, which are
424 common in Haiyan sediments (45 – 6320 foraminifera per 5 cm³ at Ba).

425 PAM cluster analysis recognized two clusters corresponding to the
426 overwash sediments derived from the mixed-carbonate environment of Basey
427 (cluster B1) and the three clastic (cluster B2) transects from Tanauan (Fig. 6b).
428 Cluster B1 (average silhouette width = 0.232) consists exclusively of Basey

429 samples, which have high concentrations of calcareous foraminifera (45 – 6320
430 foraminifera per 5 cm³) that were variably abraded and unaltered (19 – 66% and
431 26 – 64% respectively). Cluster B2 (average silhouette width = 0.140) generally
432 contained only Haiyan sediments derived from the clastic coastline near
433 Tanauan. These samples are characterized by lower concentrations of
434 calcareous foraminifera (5 – 80 foraminifera per 5 cm³) that were generally
435 more unaltered (e.g., 20 – 82% at Ma) than those from cluster B1. The Haiyan
436 sediments in Ba1, Ba2, and Ba12 clustered in B2 because of higher abundances of
437 testate amoebae (63%, 35%, and 30% respectively).

438 Two clusters within the overwash sediments at Basey (Ba) were defined
439 based on their distance along the transect (Fig. 6c). Cluster C1 (average
440 silhouette width = 0.261) corresponds to stations within 140 m of the shoreline,
441 and cluster C2 (average silhouette width = 0.414) corresponds to samples from
442 distances ranging from 160 – 340 m. The clusters were generally defined by the
443 presence of testate amoebae (0 testate amoebae per 5 cm³ in C1 vs. up to 535 per
444 5 cm³ in C2), and small foraminifera (29 – 57% (average = 41%) in C1 vs. 39 –
445 100% (average = 82%) in C2). PAM cluster analysis of the three Tanauan
446 transects (Sc, So, and Ma) produced two clusters: D1 (average silhouette width =
447 0.040) corresponding to stations within 180 m of the shoreline, and D2 (average
448 silhouette width = 0.350), corresponding to distances ranging from 400 to 1540
449 m (Fig. 6d). The overwash sediments at stations in cluster D1 are characterized
450 by the presence of agglutinated foraminifera (up to 97 individuals per 5 cm³), the
451 absence or low abundance of testate amoebae (absent except at Ma9 where, up
452 to 15 individuals of *Centropyxis* spp. were found), and large foraminifera (39 –
453 66%; average = 53%). In contrast, the overwash sediments at stations in cluster
454 D2 are characterized by a paucity of agglutinated foraminifera, higher
455 concentrations of testate amoebae (10 – 440 testate amoebae per 5 cm³), and
456 higher abundances of small foraminifera (37 – 86%; average = 64%).

457

458 6. *Microfossil characteristics of the Haiyan overwash sediments*

459 The sediments deposited by Typhoon Haiyan on coastlines of the Leyte
460 Gulf were discriminated from underlying sediments (e.g., clusters A1 and A2 on
461 Fig. 6a) based on the presence of intertidal and subtidal benthic, and planktic
462 foraminifera. At three of the four sites (Basey, Santa Cruz, and Solano),
463 calcareous species were the main constituents of the foraminiferal assemblage
464 (up to 6320 foraminifera per 5 cm³), but were generally absent in underlying
465 soils. This was especially clear with samples collected from the Tanauan
466 transects where there was a paucity of calcareous foraminifera in underlying
467 soils (except at Ma4), but up to 97 individuals per 5 cm³ in the overwash
468 sediments. This trend is in agreement with other studies that have documented
469 overwash sediments in coastal settings and have found influxes and increased
470 diversity of marine foraminifera within storm deposits (Hippensteel and Martin,
471 1999; Cochran et al., 2005; Hawkes and Horton, 2012).

472 Although the Haiyan overwash sediments could be easily discriminated
473 from the underlying soils at all sites, the contrasting environments between
474 Basey and the Tanauan transects resulted in differing microfossil assemblages
475 and two distinct PAM-defined clusters (B1: Haiyan overwash sediments from
476 Basey, B2: Haiyan overwash sediments from Tanauan; Fig. 6b). For example, in
477 the Tanauan transects (Sc, So, and Ma), the foraminiferal assemblage consists of
478 35 - 100% calcareous species, with *A. parkinsoniana* and planktics dominating
479 (at Ma, up to 57% and 87% respectively). At Basey (Ba), a protected carbonate
480 tidal flat, the overwash sediments contained abundant and diverse foraminifera
481 that are exclusively calcareous and include typical intertidal (e.g., *A.*
482 *parkinsoniana*, *A. tepida*), subtidal (e.g., *Cibicides* sp., *Pararotalia* sp.), and
483 planktic species. Mixed assemblages, containing nearshore benthics as well as
484 offshore planktics, have been reported in association with storm and tsunami
485 sediments (e.g., Dahanayake and Kulasena, 2008; Uchida et al., 2010; Hawkes
486 and Horton, 2012; Pilarczyk et al., 2012). For example, Uchida et al. (2010)
487 found a mixture of shallow- (0 – 30 m water depth) and deep-dwelling (>170 m

488 water depth) benthics, and planktic foraminifera within tsunami sediments from
489 Japan. Similarly, overwash sediments associated with the 2004 Indian Ocean
490 tsunami were composed of a mixed foraminiferal assemblage containing shallow
491 intertidal, nearshore, and planktic taxa (Nagendra et al., 2005; Hawkes et al.,
492 2007). At all sample locations, planktic species are a main constituent of the
493 Haiyan overwash sediments, with highest abundances found in Haiyan
494 sediments from Tanauan (e.g., up to 87% at Ma). Planktic foraminifera are
495 commonly found in overwash sediments and have previously been used to
496 identify and interpret storm deposits (e.g., Hippensteel and Martin, 1999;
497 Hawkes and Horton, 2012). The presence of planktic foraminifera up to the
498 landward limit of the overwash sediments may be related to their small size and
499 chamber arrangement, which is designed for floatation in the water column
500 (BouDagher-Fadel et al., 1997).

501 In addition to influxes of calcareous foraminifera, the Haiyan overwash
502 sediments could be identified by the presence of intertidal agglutinated species
503 (up to 97 per 5 cm³) at Magay. Agglutinated intertidal foraminifera (e.g., *E.*
504 *macrescens*, *M. fusca*, and *T. inflata*), characteristic of salt marsh and mangrove
505 environments (Culver, 1990; Woodroffe et al., 2005), were sourced from the
506 soils underlying the *Nypa* forest and incorporated into the overwash sediments
507 at Magay. Agglutinated mangrove foraminifera, such as those found within the
508 Haiyan overwash sediments, have also been found in association with tsunami
509 sediments elsewhere (Onuki et al., 1961; Nagendra et al., 2005; Hawkes et al.,
510 2007) and indicate scour of coastal sediments by large waves. In trench
511 sections, the concentration of agglutinated taxa within the overwash sediments
512 peaked in the upper 1 cm, possibly indicating rapid recolonization of
513 foraminifera following the typhoon (Horton et al., 2009).

514 Although testate amoebae have been used to identify freshwater
515 environments (e.g., Charman, 2001, Scott et al., 2001), they have not been used
516 to distinguish overwash sediments. Within our study area, testate amoebae are
517 abundant in underlying rice field soils (up to 11,475 individuals per 5 cm³),

518 ponds (up to 1250 individuals per 5 cm³), and grassy areas (up to 280
519 individuals per 5 cm³), with coconut groves being nearly devoid of them. Taxa
520 such as *Diffflugia* spp. and *Centropyxis* spp. were a component of the Haiyan
521 assemblage at locations where the underlying soil contained abundant testate
522 amoebae (e.g., Ba1 – Ba4, Ba10 – Ba12; Fig. 3a,b). Species of *Diffflugia* are
523 common in sediments from freshwater environments such as lakes, bogs, and
524 ponds (Medioli and Scott, 1983). Species of *Centropyxis* often have a higher
525 salinity tolerance and their ecological niche spans both freshwater and brackish
526 environments (e.g., Scott et al., 2001). In general, *Diffflugia* spp. dominated inland
527 rice field soils at our sites. Abundances of *Centropyxis* spp. increased in grassy
528 soils and pond sediments that were located closer to the coastline and influenced
529 by periodic marine inundation and salt spray.

530 Calcareous foraminifera within the overwash sediments were generally
531 larger in size (up to 71% of the assemblage was >250µm) compared to those
532 from the underlying soils. The size of individual foraminifera can be used to
533 assess the transport history of coastal sediments (e.g., Li et al., 1998; Yordanova
534 and Hohenegger, 2007; Pilarczyk and Reinhardt, 2012). This technique has
535 recently been applied to overwash sediments (e.g., Hawkes et al., 2007; Uchida et
536 al., 2010) on the basis that test size, similar to sediment grain size, is an indicator
537 of change in energy and distance of transport (e.g., Weiss, 2008).

538 Changes in the abundance of large and small test sizes contributed to
539 defining two clusters corresponding to distance from the shoreline (Fig. 6c, d).
540 In general, the test size of calcareous foraminifera within the overwash
541 sediments varied with distance inland. This trend was most pronounced at
542 Basey where an assemblage shift from large tests (>250 µm) to small tests
543 occurred at ~150 m (Fig. 3; Supplementary Table S1). Similarly, test size
544 decreased with increasing distance inland at Solano and Magay (Figs. 4, 5;
545 Supplementary Tables S2- S4). For example, the assemblage decreased from
546 56% large foraminifera closest to the shoreline at Magay to 14% at the landward
547 limit of the overwash sediments. This is similar to a study by Pilarczyk et al.

548 (2012) that documented a landward decrease in test size within the Tohoku
549 tsunami sediments from Sendai, Japan. The decrease in test size within the
550 Tohoku tsunami sediments coincided with the introduction of mud into the sand
551 deposit, which was a result of the waning energy and sustained pooling of
552 marine water. At Santa Cruz, test size decreased from 66% closest to the
553 shoreline to 36% at the most landward extent of the transect. However,
554 anomalously high abundances of large tests were found at Sc5 - Sc6 (57% and
555 61% respectively) and may be the result of pooling storm surge water in low-
556 lying areas within the rice field.

557

558 7. *Provenance of the Haiyan overwash sediments*

559 Sediments deposited by Typhoon Haiyan on coastlines of the Leyte Gulf
560 contain microfossils of subtidal, intertidal, and freshwater origin. This is to be
561 expected, because as typhoons approach a coastline, they erode, transport, and
562 deposit marine, coastal, and terrigenous sediments (Hawkes and Horton, 2012;
563 Hippensteel et al., 2013; Pilarczyk et al., 2014). The presence of foraminifera of
564 intertidal to subtidal origin suggests that a major component of the overwash
565 sediments was derived from shallow nearshore locations, with the possibility of
566 a deeper source. For example, at Basey, the overwash sediments were sourced
567 predominantly from intertidal to subtidal (*A. parkinsoniana*, *A. tepida*) sediments
568 along a protected mixed-carbonate coastline. However, the overwash sediments
569 also contained up to 13% of unaltered deeper-dwelling (up to 60 m water depth;
570 Javaux and Scott, 2003) *E. repandus*, *C. tabaensis*, and planktics. The presence of
571 these taxa indicates that the storm surge scoured not only the nearshore, but
572 also potentially deeper sediments. Deeper-dwelling microfossils have previously
573 been found in overwash deposits (e.g., Hawkes et al., 2007; Uchida et al., 2010;
574 Lane et al., 2011; Sieh et al., 2015) and assist to understand the sources for both
575 storm and tsunami sediments. Lane et al. (2011) used offshore surface transects
576 to assess the species ecology of foraminifera from northwestern Florida to

577 estimate a minimum depth of scour by storm for overwash sediments within a
578 sinkhole. Offshore species of foraminifera have been reported in nearshore
579 sediments, however, they are typically abraded and corroded and not unaltered
580 like those found within the Haiyan overwash sediments (e.g., Glenn-Sullivan and
581 Evans, 2001; Pilarczyk et al., 2011).

582 Intertidal agglutinated foraminifera (ranging from 0 – 65% of the
583 assemblage) and testate amoebae (ranging from 0 – 93% of the assemblage)
584 were also found within the overwash sediments. Due to their extensive habitat
585 range (Scott et al., 2001), which spans intertidal and virtually all inland aquatic
586 environments (e.g., Charman, 2001), testate amoebae, combined with intertidal
587 agglutinated foraminifera, can assist to identify storm overwash sediments
588 because their presence indicates terrestrial scour, transport, and mixing by the
589 storm surge. For example, Hawkes et al. (2007) used agglutinated mangrove
590 foraminifera contained within the 2004 Indian Ocean tsunami sediments to
591 identify backwash.

592 The taphonomic (or surface) character of individual foraminifera (e.g.,
593 size and patterns of abrasion, corrosion and fragmentation) has been used to
594 assess sediment provenance (e.g., Pilarczyk and Reinhardt, 2012) and, when
595 applied to overwash sediments, can provide insight into depth of scour and size
596 of event (e.g., Sieh et al., 2015). Storm and tsunami sediments often contain
597 relatively high abundances of unaltered foraminifera (e.g., Satyanarayama et al.,
598 2007; Goff et al., 2011; Pilarczyk et al., 2012; Sieh et al., 2015) because they scour
599 and deposit marine sediment from protected subtidal locations. Foraminifera
600 within the Haiyan overwash sediments are predominantly unaltered (e.g., up to
601 64% at Basey and up to 100% at Solano), suggesting that their main source was
602 not from an exposed beach or shallow intertidal areas, which would be
603 dominated by corroded and abraded individuals (Glenn-Sullivan and Evans,
604 2001; Pilarczyk et al., 2012). In an example from a carbonate reef coastline in
605 the Philippines, Glenn-Sullivan and Evans (2001) found that abraded
606 foraminifera were twice as abundant as unaltered individuals in the shallow

607 areas (<5 m of water depth). Given the shallow, gently-sloping tidal flat at Basey,
608 and the high abundances of unaltered foraminifera (up to 64% of the
609 taphonomic assemblage) within the overwash sediments, the storm surge must
610 have scoured and transported sediment from farther offshore where water
611 depths exceed 5 m.

612 *8. Conclusions*

613 In January 2014, two months after Typhoon Haiyan made landfall on the
614 Philippines, we documented the microfossil assemblages within the resulting
615 overwash sediments. Foraminiferal assemblages were used to distinguish the
616 overwash sediments from underlying soils based predominantly on the presence
617 of calcareous foraminifera such as shallow benthic species and planktics. In
618 general, underlying soils did not contain calcareous foraminifera, but rather,
619 were characterized by higher abundances of testate amoebae.

620 The Haiyan microfossil assemblage also provided information regarding
621 sediment provenance. PAM cluster analysis subdivided the Haiyan microfossil
622 dataset into two assemblages based on depositional environment: (1) a low-
623 energy mixed-carbonate tidal flat located on Samar Island (Basey transect); and
624 (2) a higher-energy clastic coastline near Tanauan on Leyte Island (Santa Cruz,
625 Solano, and Magay transects). Testate amoebae (e.g., *Centropyxis* spp., *Diffflugia*
626 spp.) and foraminifera (e.g., *A. parkinsoniana*, *A. tepida*) contained within
627 overwash sediments at each of the transects reveal up to three dominant sources
628 for the overwash sand: terrestrial, intertidal, and subtidal sources. At Basey, we
629 infer a fourth source, subtidal locations deeper than 5 m, based on the presence
630 of taphonomically unaltered deeper-dwelling species such as *E. repandus*, *C.*
631 *tabaensis*, and planktics. The presence of agglutinated mangrove foraminifera
632 and freshwater testate amoebae within the overwash sediments indicates
633 scouring, mixing, and transport of terrestrial and brackish intertidal sediments
634 by the storm surge.

635 The addition of taphonomic and test size data confirmed taxonomic
636 results that indicate a mixed source for the Haiyan overwash sediments. High
637 abundances of unaltered foraminifera within the overwash sediments suggest
638 that the main source of sediment was not from exposed intertidal areas, but
639 rather, from protected subtidal locations in excess of 5 m of water depth.

640

641 *Acknowledgements*

642 The authors would like to thank Jane Mercado (Santa Cruz), Jiggo Bermiso
643 (Magay), Carmelita Villamor (Solano), and Pelagio Tecson Jr. (Mayor of Tanauan)
644 who granted permission to conduct fieldwork on their land. Stephen Carson
645 assisted with laboratory analyses. The authors thank Jasper Knight, Briony
646 Mamo, and an anonymous reviewer for their insightful comments that improved
647 the manuscript. This work comprises Earth Observatory of Singapore
648 contribution no. 110. This research is supported by the National Science
649 Foundation (EAR 1418717), the National Research Foundation Singapore
650 (National Research Fellow Award No. NRF-RF2010-04), and the Singapore
651 Ministry of Education under the Research Centers of Excellence initiative.

652

653 *References*

654 Allen, C.R., 1962. Circum-Pacific faulting in the Philippines-Taiwan region.
655 *Journal of Geophysical Research* 67, 4795-4812.

656 Andersen, H.V., 1953. Two new species of *Haplophragmoides* from the Louisiana
657 coast. *Cushman Foundation for Foraminiferal Research Contribution* 4,
658 Washington, D.C., 21pp.

659 BouDagher-Fadel, M.K., Banner, F.T., Whittaker, J.E., 1997. Early Evolutionary
660 History of Planktonic Foraminifera. *British Micropalaeontological Society*,
661 London, 269 pp.

662 Brady, H.B., 1870. An analysis and description of the foraminifera. In: Brady,
663 G.S., Robertson, D., The ostracodes and foraminifera of tidal rivers v. 6., Annals
664 and Magazine of Natural History, London, England, 500pp.

665 Brandon, C.M., Woodruff, J.D., Lane, D.P., Donnelly, J.P., 2013. Tropical cyclone
666 wind speed constraints from resultant storm surge deposition: A 2500 year
667 reconstruction of hurricane activity from St. Marks, FL. *Geochemistry,*
668 *Geophysics, Geosystems* 14, 2993-3008.

669 Charman, D.J., 2001. Biostratigraphic and palaeoenvironmental applications of
670 testate amoebae. *Quaternary Science Reviews* 20, 1753-1764.

671 Clark, K., Cochran, U., Mazengarb, C., 2011. Holocene coastal evolution and
672 evidence for paleotsunami from a tectonically stable region, Tasmania, Australia.
673 *The Holocene* 21, 883-895.

674 Cochran, U.A., Berryman, K.R., Middenhall, D.C., Hayward, B.W., Southall, K.,
675 Hollis, C.J., 2005. Towards a record of Holocene tsunami and storms from
676 northern Hawke's Bay, New Zealand. *New Zealand Journal of Geology and*
677 *Geophysics* 48, 507-515.

678 Collins, A.C., 1958. Foraminifera. Great Barrier Reef Expedition 1928-1929.
679 *Scientific Reports. Vol. 6, British Museum of Natural History, London, 414pp.*

680 Collins, E.S., Scott, D.B., Gayes, P.T., 1999. Hurricane records on the South
681 Carolina coast: can they be detected in the sediment record? *Quaternary*
682 *International* 56, 15-26.

683 Culver, S.J., 1990. Benthic foraminifera of Puerto Rican mangrove-lagoon
684 systems: potential for palaeoenvironmental interpretations. *Palaios* 5, 34-51.

685 Cushman, J.A., 1926. Recent foraminifera from Puerto Rico. Carnegie Institute
686 Washington, Publication no. 344, Washington, D.C., 344pp.

687 Dahanayake, K., Kulasena, N., 2008. Recognition of diagnostic criteria for recent-
688 and paleo-tsunami sediments from Sri Lanka. *Marine Geology* 254, 180-186.

689 Debenay, J.-P., 2013. A guide to 1,000 foraminifera from southwestern Pacific,
690 New Caledonia. IRD Éditions, Publications scientifiques du Muséum national
691 d'Histoire naturelle, Paris, France, 384 pp.

692 Denommee, K.C., Bentley, S.J., Droxler, A.W., 2014. Climatic controls on hurricane
693 patterns: a 1200-y near-annual record from Lighthouse Reef, Belize. *Scientific*
694 *Reports* 4, 3876, doi: 10.1038/srep03876.

695 Dominey-Howes, D., Cundy, A., Croudace, I., 2000. High energy marine flood
696 deposits on Astypalaea Island, Greece: possible evidence for the AD 1956
697 southern Aegean tsunami. *Marine Geology* 163, 303-315.

698 Donnelly, J.P., Hawkes, A.D., Lane, P., MacDonald, D., Shuman, B.N., Toomey, M.R.,
699 van Hengstum, P.J., Woodruff, J.D., 2015. Climate forcing of unprecedented
700 intense-hurricane activity in the last 2000 years. *Earth's Future* 3, 49-65.

701 Donnelly, J.P., Roll, S., Wengren, M., Butler, J., Lederer, R., Webb, T., 2001.
702 Sedimentary evidence of intense hurricane strikes from New Jersey. *Geology* 29,
703 615-618.

704 d'Orbigny, A., 1839. Foraminiferes. In: Ramon de la Sagra, *Histoire physique et*
705 *naturelle de l'île de Cuba*. A. Bertrand, Paris, France, 454pp.

706 Duquesnoy, T., Barrier, E., Kasser, M., Aurelio, M.A., Gaulon, R., Punongbayan, R.S.,
707 Rangin, C., 1994. Detection of creep along the Philippine Fault: first results of
708 geodetic measurements on Leyte Island, central Philippine. *Geophysical*
709 *Research Letters* 21, 975-978.

710 Fichtel, L., Moll, J.P.C., 1798. *Testacea microscopica aliaque minuta ex generibus*
711 *Argonauta et Nautilus* (Microscopische und andere kleine Schalthiere aus den
712 Geschlechtern Argonaute und Schiffer). Anton Pichler, Vienna, 124pp.

713 Garcia-Herrera, R., Ribera, P., Hernandez, E., Gimeno, L., 2007. Northwest Pacific
714 typhoons documented by the Philippine Jesuits, 1566-1900. *Journal of*
715 *Geophysical Research* 112, D06108, doi: 10.1029/2006JD007370.

716 Glenn-Sullivan, E.C., Evans, I., 2001. The effects of time-averaging and
717 taphonomy on the identification of reefal sub-environments using larger
718 foraminifera: Apo Reef, Mindoro, Philippines. *Palaios* 16, 399-408.

719 Goff, J., Lamarche, G., Pelletier, B., Chagué-Goff, C., Strotz, L., 2011. Predecessors
720 to the 2009 South Pacific tsunami in the Wallis and Futuna archipelago. *Earth-*
721 *Science Reviews* 107, 91-106.

722 Hart, J., Hearn, G., Chant, C., 2002. Engineering on the precipice: mountain road
723 rehabilitation in the Philippines. *Quaternary Journal of Engineering Geology and*
724 *Hydrogeology* 35, 223-231.

725 Hawkes, A.D., Bird, M., Cowie, S., Grund-Warr, C., Horton, B.P., Shau Hwai, A.T.,
726 Law, L., Macgregor, C., Nott, J., Ong, J.E., Rigg, J., Robinson, R., Tan-Mullins, M.,
727 Tiong Sa, T., Yasin, Z., Aik, L.W., 2007. Sediments deposited by the 2004 Indian
728 Ocean tsunamis along the Malaysia-Thailand Peninsula. *Marine Geology* 242,
729 169-190.

730 Hawkes, A.D., Horton, B.P., 2012. Sedimentary record of storm deposits from
731 Hurricane Ike, Galveston and San Luis Islands, Texas. *Geomorphology* 171, 180-
732 189.

733 Hayward, B.W., Holzmann, M., Grenfell, H.R., Pawlowski, J., Triggs, C.M., 2004.
734 Morphological distinction of molecular types in *Ammonia* – towards a taxonomic
735 revision of the world's most commonly misidentified foraminifera. *Marine*
736 *Micropaleontology* 50, 237-271.

737 Hewins, M.R., Perry, C.T., 2006. Bathymetric and environmentally influenced
738 patterns of carbonate sediment accumulation in three contrasting reef settings,
739 Danjungan Island, Philippines. *Journal of Coastal Research* 22, 812-824.

740 Hippensteel, S.P., Martin, R.E., 1999. Foraminifera as an indicator of overwash
741 deposits, barrier island sediment supply, and barrier island evolution: Folly
742 Island, South Carolina. *Palaeogeography Palaeoclimatology Palaeoecology* 149,
743 115-125.

744 Hippensteel, S.P., Eastin, M.D., Garcia, W.J., 2013. The geological legacy of
745 Hurricane Irene: implications for the fidelity of the paleo-storm record. *GSA*
746 *Today* 23, 4-10.

747 Hippensteel, S.P., Martin, R.E., Harris, M.S., 2005. Discussion: Records of
748 prehistoric hurricanes on the South Carolina coast based on
749 micropaleontological and sedimentological evidence, with comparison to other
750 Atlantic Coast records. *Geological Society of America Bulletin* 117, 250-256.

751 Horton, B.P., Rossi, V., Hawkes, A.D., 2009. The sedimentary record of the 2005
752 hurricane season from the Mississippi and Alabama coastlines. *Quaternary*
753 *International* 195, 15-30.

754 Javaux, E.J., Scott, D.B., 2003. Illustration of modern benthic foraminifera from
755 Bermuda and remarks on distribution in other subtropical/tropical areas.
756 *Palaeontologia Electronica* 6, 22 pp, [http://palaeo-](http://palaeo-electronica.org/2003_1/benthic/issue1_03.htm)
757 [electronica.org/2003_1/benthic/issue1_03.htm](http://palaeo-electronica.org/2003_1/benthic/issue1_03.htm).

758 Joint Typhoon Warning Center, 2014. JTWC Western North Pacific best track
759 data 2013. Available online at [http://www.usno.navy.mil/](http://www.usno.navy.mil/NOOC/nmfcph/RSS/jtwc/best_tracks/wpindex.php)
760 [NOOC/nmfcph/RSS/jtwc/best_tracks/wpindex.php](http://www.usno.navy.mil/NOOC/nmfcph/RSS/jtwc/best_tracks/wpindex.php)

761 Kaufman, L., Rousseeuw, P.J., 1990. *Finding Groups in Data: An Introduction to*
762 *Cluster Analysis*. Wiley-Interscience, California, 368 pp.

763 Kemp, A.C., Horton, B.P., Vann, D.R., Engelhart, S.E., Grand Pre, C.A., Vane, C.H.,
764 Nikitina, D., Anisfeld, S.C., 2012. Quantitative vertical zonation of salt-marsh
765 foraminifera for reconstructing former sea level: an example from New Jersey,
766 USA. *Quaternary Science Reviews* 54, 26-39.

767 Kortekaas, S., Dawson, A.G., 2007. Distinguishing tsunami and storm deposits:
768 An example from Martinhal, SW Portugal. *Sedimentary Geology* 200, 208-221.

769 Lacuna, M.L.D.G., Alviro, M.P., 2014. Diversity and abundance of benthic
770 foraminifera in nearshore sediments of Iligan City, Northern Mindanao,
771 Philippines. *ABAH Bioflux* 6, 10-26.

772 Lacuna, M.L.D.G., Masangcay, S.I.G., Orbita, M.L.S., Torres, M.A.J., 2013.
773 Foraminiferal assemblage in southeast coast of Iligan Bay, Mindanao, Philippines.
774 *AAAL Bioflux* 6, 303-319.

775 Landsea, C.W., Harper, B.A., Hoarau, K., Knaff, J.A., 2006. Can we detect trends in
776 extreme tropical cyclones? *Science* 313, 452-454.

777 Lane, P., Donnelly, J.P., Woodruff, J.D., Hawkes, A.D., 2011. A decadal-resolved
778 paleohurricane record archived in the late Holocene sediments of a Florida
779 sinkhole. *Marine Geology* 287, 14-30.

780 Li, C., Jones, B., Kalbfleisch, W.B.C., 1998. Carbonate sediment transport
781 pathways based on foraminifera: case study from Frank Sound, Grand Cayman,
782 British West Indies. *Sedimentology* 45, 109-120.

783 Lin, I.I., Black, P., Price, J.F., Yang, C.-Y., Chen, S.S., Lien, C.-C., Harr, P., Chi, N.-H.,
784 Wu, C.-C., D'Asaro, E.A., 2013. An ocean coupling potential intensity index for
785 tropical cyclones. *Geophysical Research Letters* 40, 1878-1882.

786 Liu, K.B., Fearn, M.L., 1993. Lake-sediment record of late Holocene hurricane
787 activities from coastal Alabama. *Geology* 21, 793-796.

788 Liu, K.B., Fearn, M.L., 2000. Reconstruction of prehistoric landfall frequencies of
789 catastrophic hurricanes in northwestern Florida from lake sediment records.
790 *Quaternary Research* 54, 238-245.

791 Loeblich, A.R., Tappan, H., 1987. Foraminiferal genera and their classification.
792 Van Nostrand Rienhold Co., New York, I-II.

793 Maechler, M., Rousseeuw, P., Struyf, A., Hubert, M., 2005. Cluster Analysis Basics
794 and Extensions, Available at: URL [http://cran.r-project.org/web/](http://cran.r-project.org/web/packages/cluster/index.html)
795 [packages/cluster/index.html](http://cran.r-project.org/web/packages/cluster/index.html)

796 Medioli, F.S., Scott, D.B., 1983. Holocene Arcellacea (thecamoebians) from
797 Eastern Canada. Cushman Foundation for Foraminiferal Research Special
798 Publication 21, 1-63.

799 Montagu, G., 1808. Supplement to Testacea Britannica, Exeter, England, 81pp.

800 Mori, N., Kato, M., Kim, S., Mase, H., Shibutani, Y., Takemi, T., Tsuboki, K., Yasuda,
801 T., 2014. Local amplification of storm surge by super typhoon Haiyan in Leyte
802 Gulf. Geophysical Research Letters 41, 5106-5113.

803 Nagendra, R., Kannan, B.V.K., Sajith, C., Sen, G., Reddy, A.N., Srinivasalu, S., 2005.
804 A record of foraminiferal assemblage in tsunami sediments along Nagappattinam
805 coast, Tamil Nadu. Current Science 89, 1947-1952.

806 NDRRMC (National Disaster Risk Reduction and Management Council), 2014.
807 SitRep No. 27 Effects of Typhoon "Ruby" (Hagupit), 19 December 2014, Available
808 at: www.ndrrmc.gov.ph.

809 Nguyen, P., Sellars, S., Thorstensen, A., Tao, Y., Ashouri, H., Braithwaite, D., Hsu,
810 K., Sorooshian, S., 2014. Satellites track precipitation of Super Typhoon Haiyan.
811 EOS Transactions 95, 133-135.

812 Ogden, C.G., Hedley, R.H., 1980. An atlas of freshwater testate amoebae. Oxford
813 University Press, New York, 222 pp.

814 Onuki, Y., Shibata, T., Mii, H., 1961. Coastal region between Taro and Kamaishi.
815 In: Kon'no, E. (Ed.), Geological observations of the Sanriku coastal region
816 damaged by the tsunami due to the Chile earthquake in 1969. Contributions
817 from the Institute of Geology and Paleontology, Tohoku University, Sendai, pp.
818 16-27.

819 Otvos, E.F., 1999. Quaternary coastal history, basin geometry and assumed
820 evidence for hurricane activity, northeastern Gulf of Mexico coastal plain.
821 Journal of Coastal Research 15, 438-443.

822 Perelis, L., Reiss, Z., 1976. *Cibicididae*. In: Recent sediments from the Gulf of Elat.
823 Israel Journal of Earth Science, Jerusalem, Israel 24, 78pp.

824 Pilarczyk, J.E., Dura, T., Horton, B.P., Engelhart, S.E., Kemp, A.C., Sawai, Y., 2014.
825 Microfossils from coastal environments as indicators of paleo-earthquakes,
826 tsunamis and storms. Palaeogeography, Palaeoclimatology, Palaeoecology 413,
827 144-157.

828 Pilarczyk, J.E., Horton, B.P., Witter, R.C., Vane, C.H., Chagué-Goff, C., Goff, J., 2012.
829 Sedimentary and foraminiferal evidence of the 2011 Tohoku-oki tsunami on the
830 Sendai coastal plain, Japan. Sedimentary Geology 282, 78-89.

831 Pilarczyk, J.E., Reinhardt, E.G., 2012. *Homotrema rubrum* (Lamarck) taphonomy
832 as in overwash indicator in Marine Ponds on Anegada, British Virgin Islands.
833 Natural Hazards 63, 85-100.

834 Pilarczyk, J.E., Reinhardt, E.G., Boyce, J.I., Schwarcz, H.P., Donato, S.V., 2011.
835 Assessing surficial foraminiferal distributions as an overwash indicator in Sur
836 Lagoon, Sultanate of Oman. Marine Micropaleontology 80, 62-73.

837 Pun, I.-F., Lin, I.-I., Lo, M.-H., 2013. Recent increase in high tropical cyclone heat
838 potential area in the Western North Pacific Ocean. Geophysical Research Letters
839 40, 4680-4684.

840 Rabien, K.A., Culver, S.J., Buzas, M.A., Corbett, D.R., Walsh, J.P., Tichenor, H.R.,
841 2015. The foraminiferal signature of recent Gulf of Mexico hurricanes. Journal of
842 Foraminiferal Research 45, 82-105.

843 Ribera, P., Garcia-Herrera, R., Gimeno, L., 2008. Historical deadly typhoons in the
844 Philippines. Weather 63, 194-199.

845 Satyanarayana, K., Reddy, A.N., Jaiprakash, B.C., Chidambaram, L., Srivastava, S.,
846 Bharktya, D.K., 2007. A note on foraminifera, grain size and clay mineralogy of
847 tsunami sediments from Karaikal-Nagore-Nagapattinam Beaches, Southeast
848 Coast of India. *Journal Geological Society of India* 69, 70-74.

849 Scott, D.B., Collins, E.S., Gayes, P.T., Wright, E., 2003. Records of prehistoric
850 hurricanes on the South Carolina coast based on micropaleontological and
851 sedimentological evidence, with comparison to other Atlantic Coast records.
852 *Geological Society of America Bulletin* 115, 1027-1039.

853 Scott, D.B., Medioli, F.S., Schafer, C.T., 2001. *Monitoring in coastal environments*
854 *using foraminifera and thecamoebian indicators.* Cambridge University Press,
855 Cambridge, 177pp.

856 Sieh, K., Daly, P., McKinnon, E.E., Pilarczyk, J.E., Chiang, H.W., Horton, B., Rubin,
857 C.M., Shen, C.C., Ismail, N., Vane, C.H., Feener, R.M., 2015. Penultimate
858 predecessors of the 2004 Indian Ocean tsunami in Aceh, Sumatra: Stratigraphic,
859 archeological, and historical evidence. *Journal of Geophysical Research - Solid*
860 *Earth* 120, 308-325.

861 Smith, H.G., Bobrov, A., Lara, E., 2008. Diversity and biogeography of testate
862 amoebae. *Biodiversity and Conservation* 17, 329-343.

863 Soria, J.L.A., Switzer, A.D., Pilarczyk, J.P., Siringan, F.P., Doctor, A., Khan, N., Fritz,
864 H.M., Ramos, R.D., Ildefonso, S.R., Garcia, M., 2016a. Sedimentary record of the
865 2013 Typhoon Haiyan deposit in the Leyte Gulf, Philippines. *European*
866 *Geosciences Union (EGU) Meeting, Vienna, Austria, 2016, abstract #EGU2016-*
867 *260.*

868 Soria, J.L.A., Switzer, A.D., Villanoy, C.L., Fritz, H.M., Bilgera, P.H.T., Cabrera, O.C.,
869 Siringan, F.P., Yacat-Sta. Maria, Y., Ramos, R.D., Fernandez, I.Q., 2016b. Repeat
870 storm surge disasters of Typhoon Haiyan and its 1897 predecessor in the
871 Philippines. *Bulletin of the American Meteorological Society* 97, 31-48.

872 Strotz, L.C., Mamo, B.L., 2009. Can foraminifera be used to identify storm
873 deposits in shallow-water tropical reef settings?: Examining the impact of
874 Cyclone Hamish on the foraminiferal assemblages of Heron Island, Great Barrier
875 Reef, Australia. American Geophysical Union, Fall Meeting 2009, abstract
876 #NH43B-1311.

877 Suerte, L.O., Yumul, G.P.Jr., Tamayo, R.A.Jr., Dimalanta, C.B., Zhou, M.-F., Maury,
878 R.C., Polvé, M., Balce, C.L., 2005. Geology, Geochemistry and U-Pb SHRIMP age of
879 the Tacloban Ophiolite Complex, Leyte (Central Philippines): Implications for the
880 existence and extent of the Proto-Philippine Sea Plate. *Resource Geology* 55,
881 207-216.

882 Tajima, Y., Yasuda, T., Pacheco, B.M., Cruz, E.C., Kawasaki, K., Nobuoka, H.,
883 Miyamoto, M., Asano, Y., Arikawa, T., Ortigas, N.M., Aquino, R., Mata, W., Valdez, J.,
884 Briones, F., 2014. Initial report of JSCE-PICE joint survey on the storm surge
885 disaster caused by Typhoon Haiyan. *Coastal Engineering Journal* 56, 1450006,
886 doi: 10.1142/S0578563414500065.

887 Travaglia, C., Baes, A.F., Tomas, L.M., 1978. Geology of Samar Island: annex 6 of
888 Samar Island reconnaissance land resources survey of priority strips for
889 integrated rural development. United Nations Development Programme, Manila,
890 149pp.

891 Uchida, J., Fujiwara, O., Hasegawa, S., Kamataki, T., 2010. Sources and
892 depositional processes of tsunami deposits: analysis using foraminiferal tests
893 and hydrodynamic verification. *Island Arc* 19, 427-442.

894 Weiss, R., 2008. Sediment grains moved by passing tsunami wave: tsunami
895 deposits in deep water. *Marine Geology* 250, 251-257.

896 Williams, H.F.L., 2009. Stratigraphy, sedimentology, and microfossil content of
897 Hurricane Rita storm surge deposits in southwest Louisiana. *Journal of Coastal*
898 *Research* 25, 1041-1051.

899 Woodroffe, S.A., Horton, B.P., Larcombe, P., Whittaker, J.E., 2005. Intertidal
900 mangrove foraminifera from the central Great Barrier Reef shelf, Australia:
901 implications for sea-level reconstruction. *Journal of Foraminiferal Research* 35,
902 259-270.

903 Yordanova, E.K., Hohenegger, J.H., 2007. Studies on settling, traction and
904 entrainment of larger benthic foraminiferal tests: implications for accumulation
905 in shallow marine sediments. *Sedimentology* 54, 1273-1306.

906 *Figure captions*

907 **Fig. 1.** (a) Location map of the Philippines showing track of Typhoon Haiyan
908 (blue dotted line). Major changes in typhoon intensity are indicated in blue and
909 are expressed as Saffir-Simpson categories. (b) Map of the Leyte Gulf indicating
910 location of Tacloban (blue shaded area), transects Ba – Ma, and Typhoon
911 Haiyan's track (JTWC, 2014). (c - d) Detailed map of Ba (Basey), Sc (Santa Cruz),
912 So (Solano), and Ma (Magay) indicating sample locations and major
913 geomorphological features.

914 **Fig. 2.** Scanning Electron Microscope (SEM) images of dominant taxa and
915 taphonomic characters. All scale bars are equal to 100 μm . (1-2) *Ammonia*
916 *convexa*, (3-4) *Ammonia parkinsoniana*, (5-6) *Ammonia tepida*, (7) *Elphidium*
917 *striatopunctatum*, (8) *Pararotalia* sp., (9) *Trochammina inflata*, (10) *Entzia*
918 *macrescens*, (11) *Centropyxis* spp., (12) *Diffugia* spp. Taphonomic states of
919 *Ammonia*: unaltered (13), abraded (14-15), and fragmented (16).

920

921 **Fig. 3.** Changes in the microfossil assemblage with increasing distance inland for
922 Ba (Basey). (a) Elevation profile indicating major geomorphological features,
923 location of sample sites (black circle), and thickness of the overwash sediments.
924 (b) Presence vs. absence of testate amoebae and foraminifera (calcareous and
925 agglutinated) for each sample location. (c) Concentration of foraminifera per 5

926 cm³. (d – e) Relative abundances of dominant foraminiferal species within the
927 overwash sediments. (f) Taphonomic condition of calcareous foraminifera. An
928 individual foraminifera can be both abraded and fragmented. (g) Abundances of
929 small and large tests within the overwash sediments. Bar graphs are stacked
930 histograms.

931 **Fig. 4.** Changes in the microfossil assemblage with increasing distance inland for
932 (a) Sc (Santa Cruz) and (b) So (Solano). (i) Elevation schematic indicating major
933 geomorphological features, location of sample sites (black circle), and thickness
934 of the overwash sediments. (ii) Presence vs. absence of testate amoebae and
935 foraminifera (calcareous and agglutinated) for each sample location. (iii)
936 Concentration of foraminifera per 5 cm³. (iv – v) Relative abundances of
937 dominant foraminiferal species within the overwash sediments. (vi)
938 Taphonomic condition of calcareous foraminifera. An individual foraminifera
939 can be both abraded and fragmented. (vii) Abundances of small and large tests
940 within the overwash sediments. Bar graphs are stacked histograms.

941 **Fig. 5.** (a) Changes in the microfossil assemblage with increasing distance inland
942 for Ma (Magay). (i) Elevation schematic indicating major geomorphic features,
943 locations of surface (black circle) and trench (thick black line) sample sites, and
944 thickness of the overwash sediments. (ii) Presence vs. absence of testate
945 amoebae and foraminifera (calcareous and agglutinated) for each sample
946 location. (iii) Concentration of foraminifera per 5 cm³. (iv) Relative abundances
947 of dominant foraminiferal species within the overwash sediments. (v)
948 Taphonomic condition of calcareous foraminifera. An individual foraminifera
949 can be both abraded and fragmented. (vi) Abundances of small and large tests
950 within the overwash sediments. The spatial gap between Ma9 and Ma10
951 corresponds to the village boundary where storm sediments accumulated over
952 paved surfaces, but did not preserve (b) Trench sections (Ma4, Ma6, and Ma9) in
953 the *Nypa* forest. Bar graphs are stacked histograms.

954 **Fig. 6.** Results of PAM cluster analysis indicating average silhouette width of
955 clustered data. For each scenario, two clusters produced the highest average
956 silhouette width (indicated by dashed vertical line) indicating the data can be
957 reliably divided into two clusters. (a) Discriminating between the overwash
958 sediments and underlying sedimentary layer. Overwash sediment samples are
959 indicated in yellow and underlying “pre-storm” sediments are indicated in
960 brown. (b) Distinguishing between the overwash sediments at a mixed-
961 carbonate site (Ba) and a clastic site (Sc, So, and Ma). Distance controlled
962 clusters within overwash sediments at Ba (c) and the Tanauan transects (d).
963 Distances from the shoreline for each cluster are indicated.

964

965

966

967

968

969

970

971

972

973

974

975

976

977

978

Figure 1

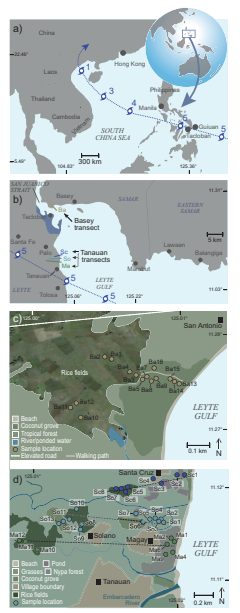


Figure 2

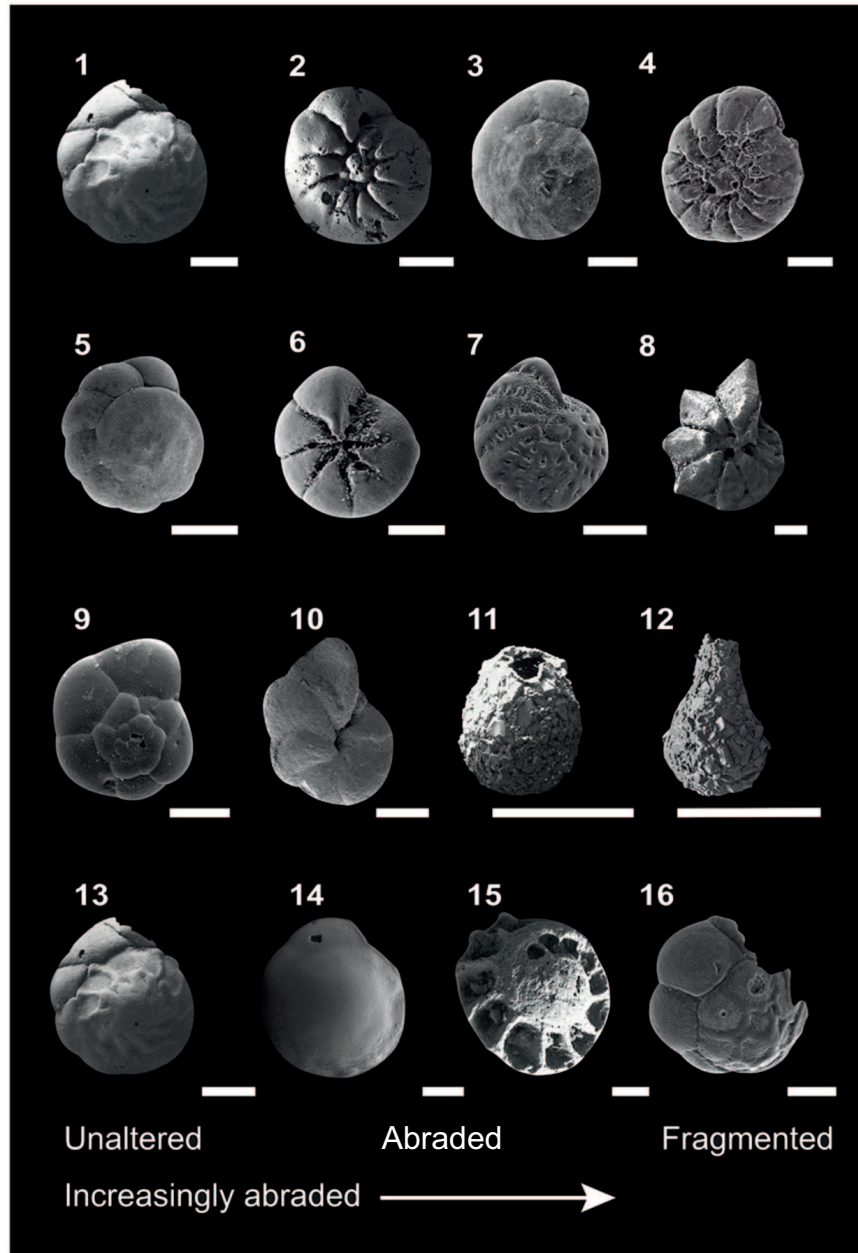


Figure 3
Basey transect (Ba)

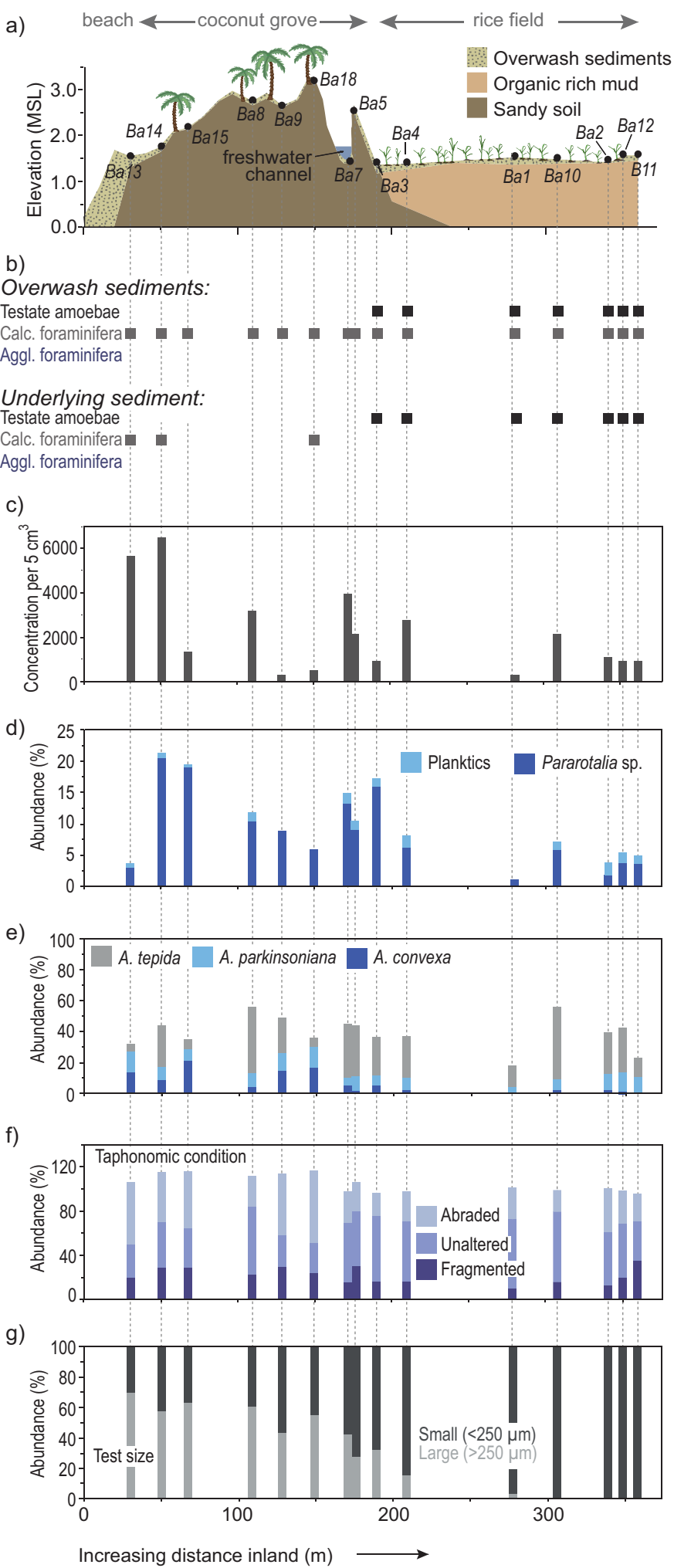
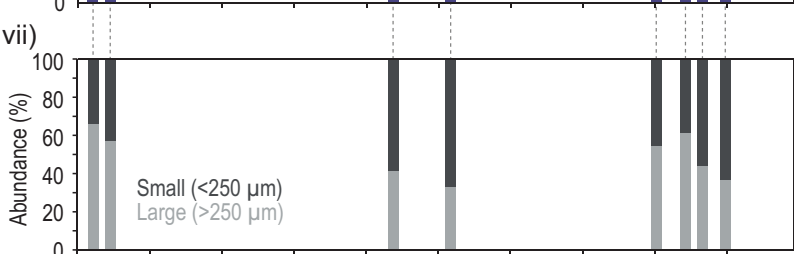
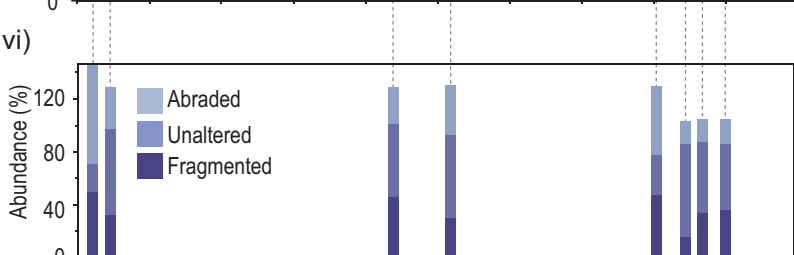
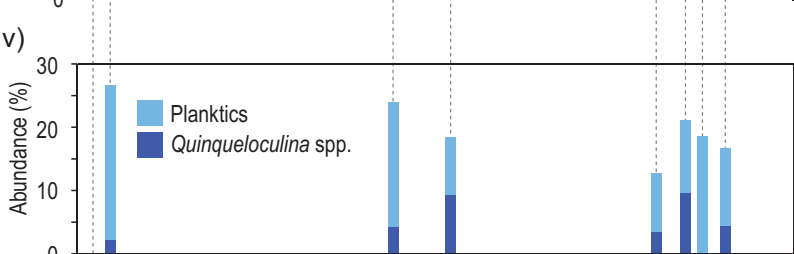
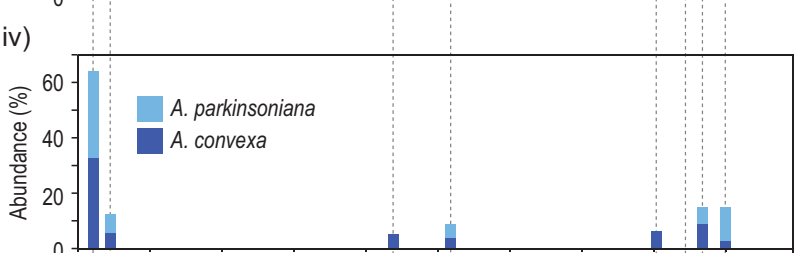
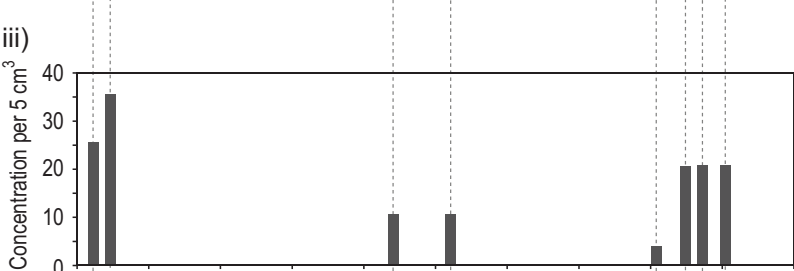
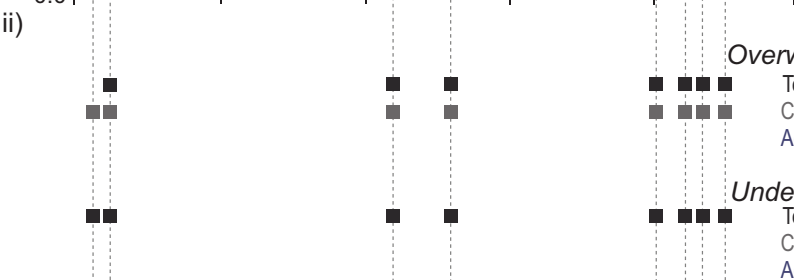
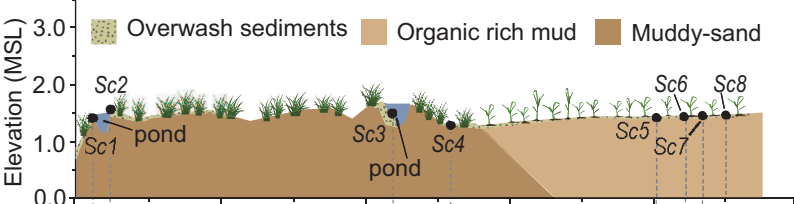


Figure 4**a) Santa Cruz transect (Sc)**

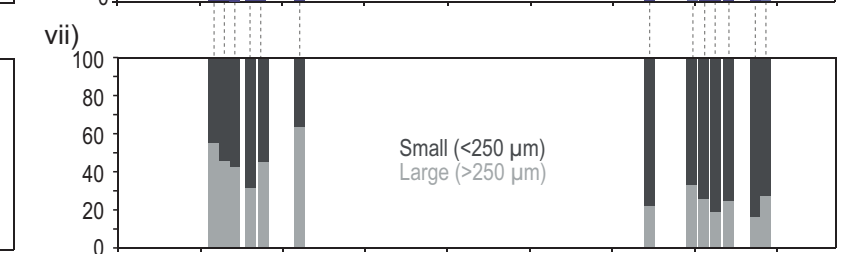
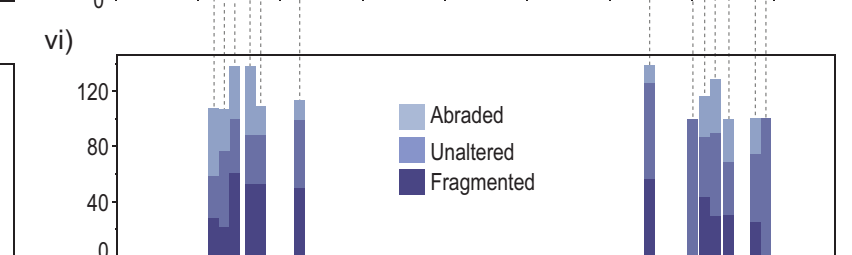
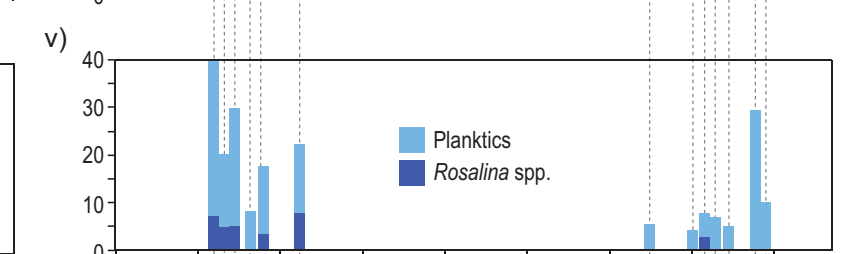
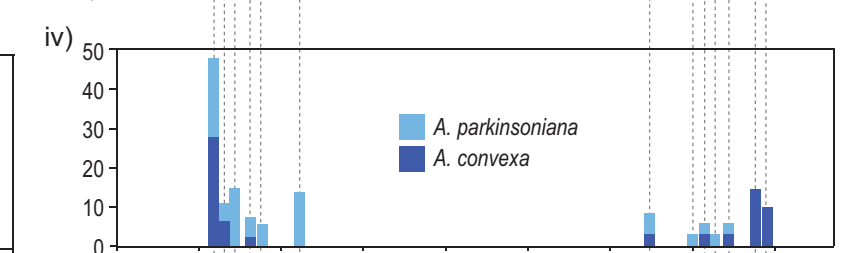
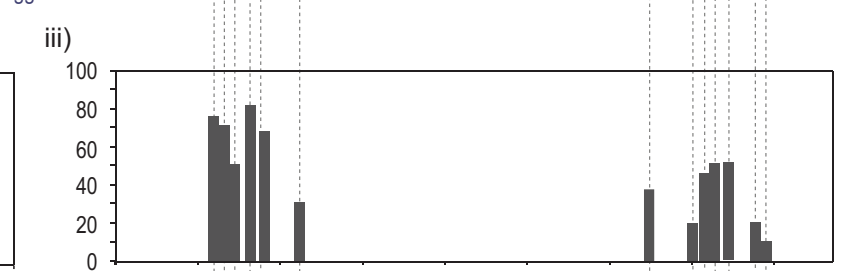
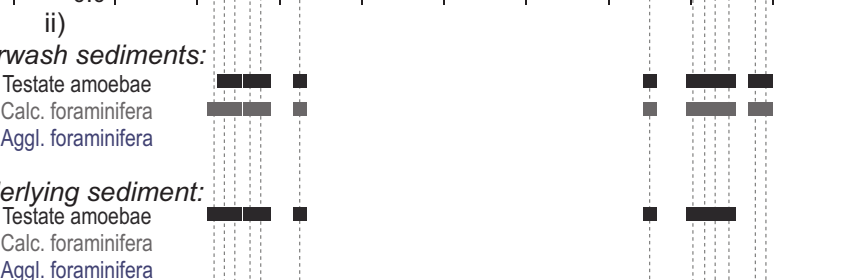
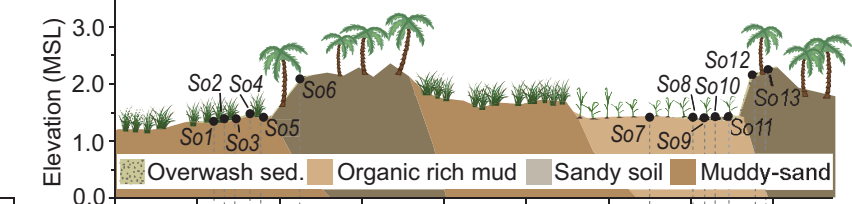
i) beach ← grasses → rice field →



Increasing distance inland (m) →

b) Solano transect (So)

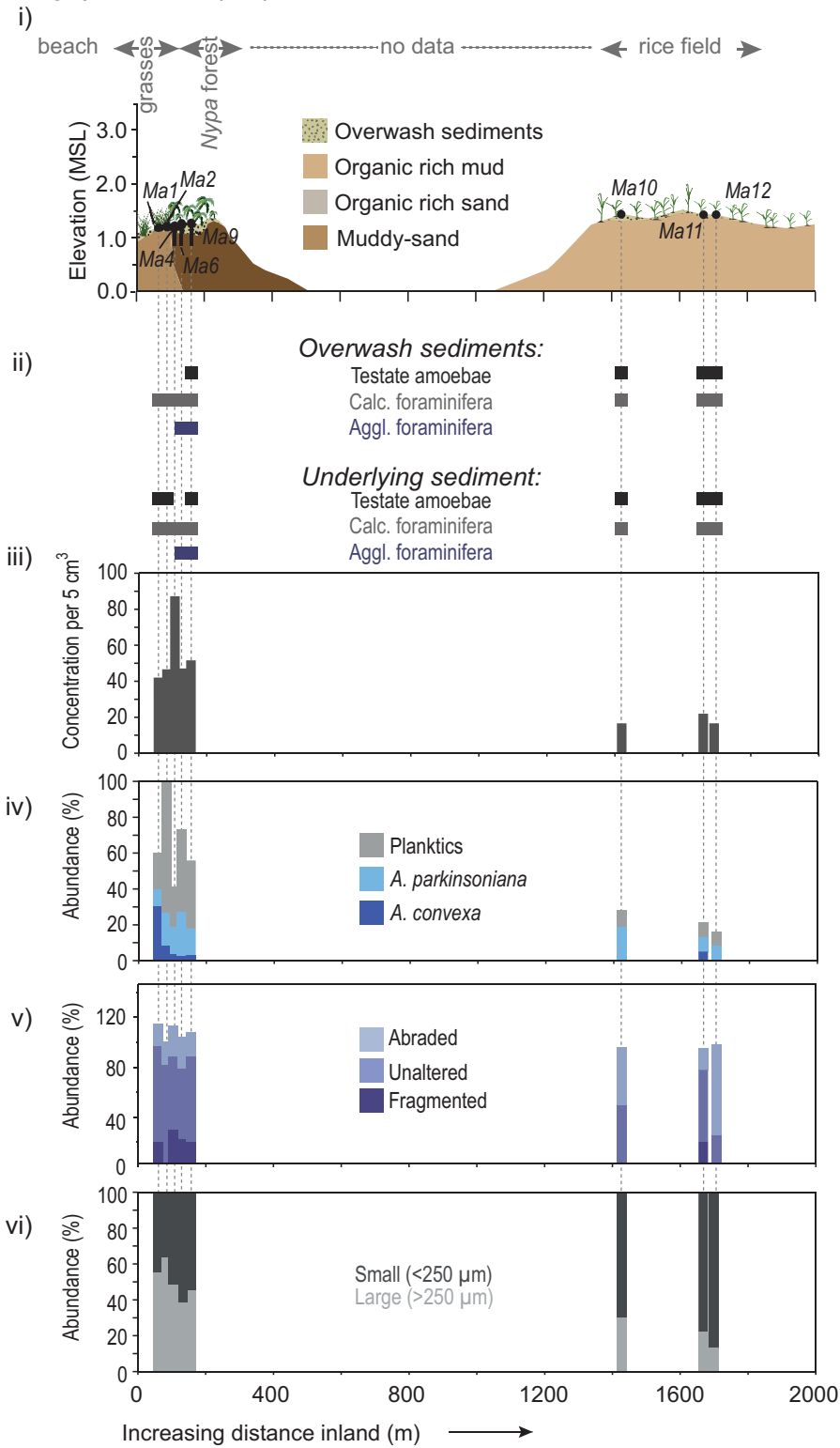
i) beach ← grasses → coconut grove → grasses → rice field → coconut grove →



Increasing distance inland (m) →

Figure 5

a) Magay transect (Ma)



b) Magay trench sections (Ma)

